National Aeronautics and Space Administration

Pyroelectric Instrument for Rock Analysis

PI: Christopher Heirwegh (322)
Co-Is: Kyle Uckert (398I), Robert Hodyss (322), Abigail Allwood (320)
Program: Topical

Introduction and Objectives:

X-ray fluorescence (XRF) instrumentation on spacecraft provides reliable whole rock elemental composition information for **planetary science** investigations.

Pyroelectricity – Temperature change **(ΔT)** applied to polarized (±z) crystals ($LiTaO_3$) breaks down polarization allowing surface charge to flow. Charge build-up on z faces discharges electrons (e^-) across gap (Fig. 1).[1] Impact on opposite face produces bremsstrahlung **X-ray emission** (eg. spectrum, Fig. 2). Reversing temperature **(-ΔT)** reverses emission direction.

The prototype **P**yroelectric **I**nstrument for **R**ock **Ana**lysis (PIRANA) is an X-ray source developed in this topical R&TD task as an alternative to existing X-ray devices, eg. PIXL and APXS. Pyroelectric devices, examined[2–4] as potential X-ray sources for elemental analysis, have been developed commercially (eg. Amptek Cool-X)[5] and for use on exploratory space craft.[6]

Objectives: Characterize 2-crystal design (Fig. 1) to **maximize flux**, **upper energy** limit (**E_{max}**) and emission **stability**, inform future design iterations, develop automated software (Fig. 3) and generate code for whole-rock geo-chemical quantification.

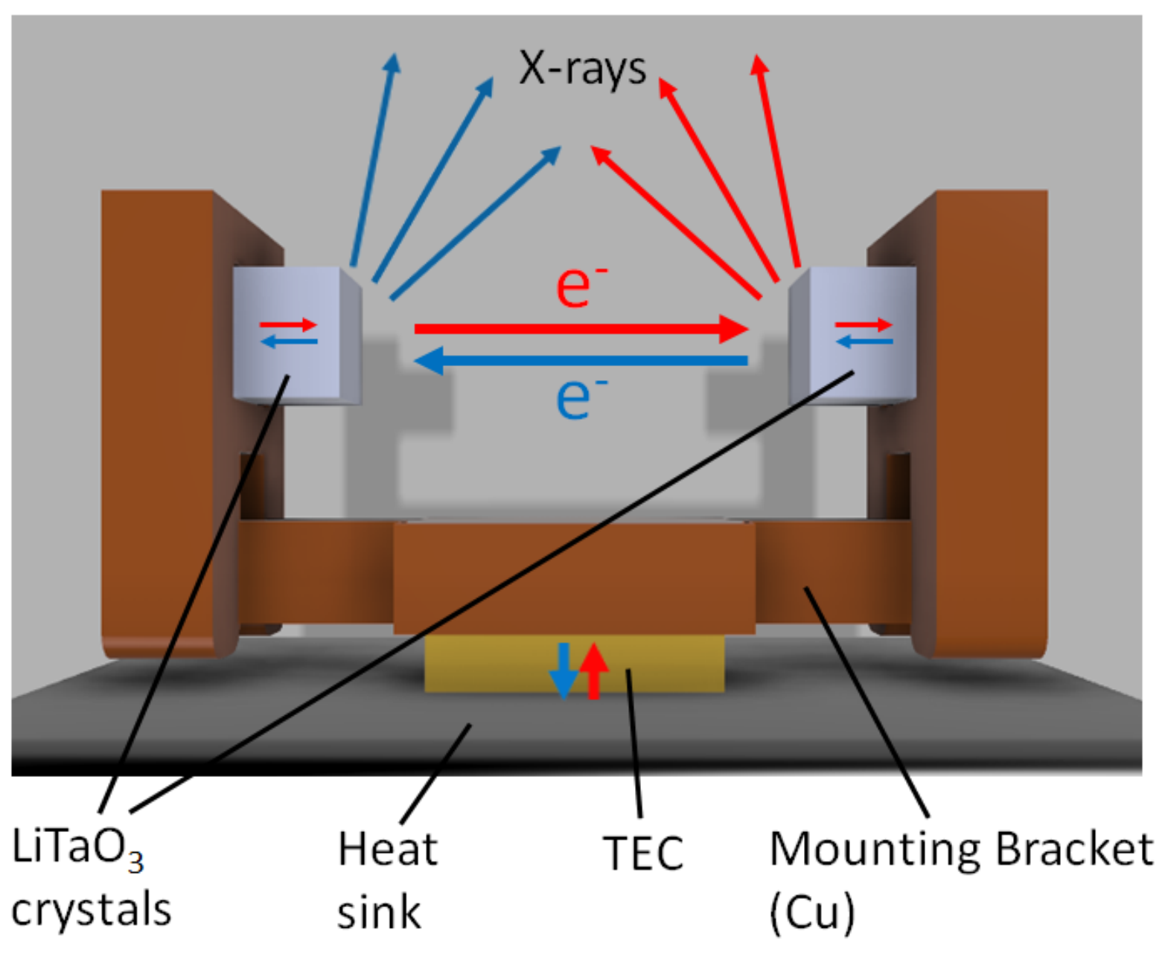

Figure 1: Schematic of 2-crystal mount showing direction of heat, electron and X-ray propagation relative to heating and cooling cycles.

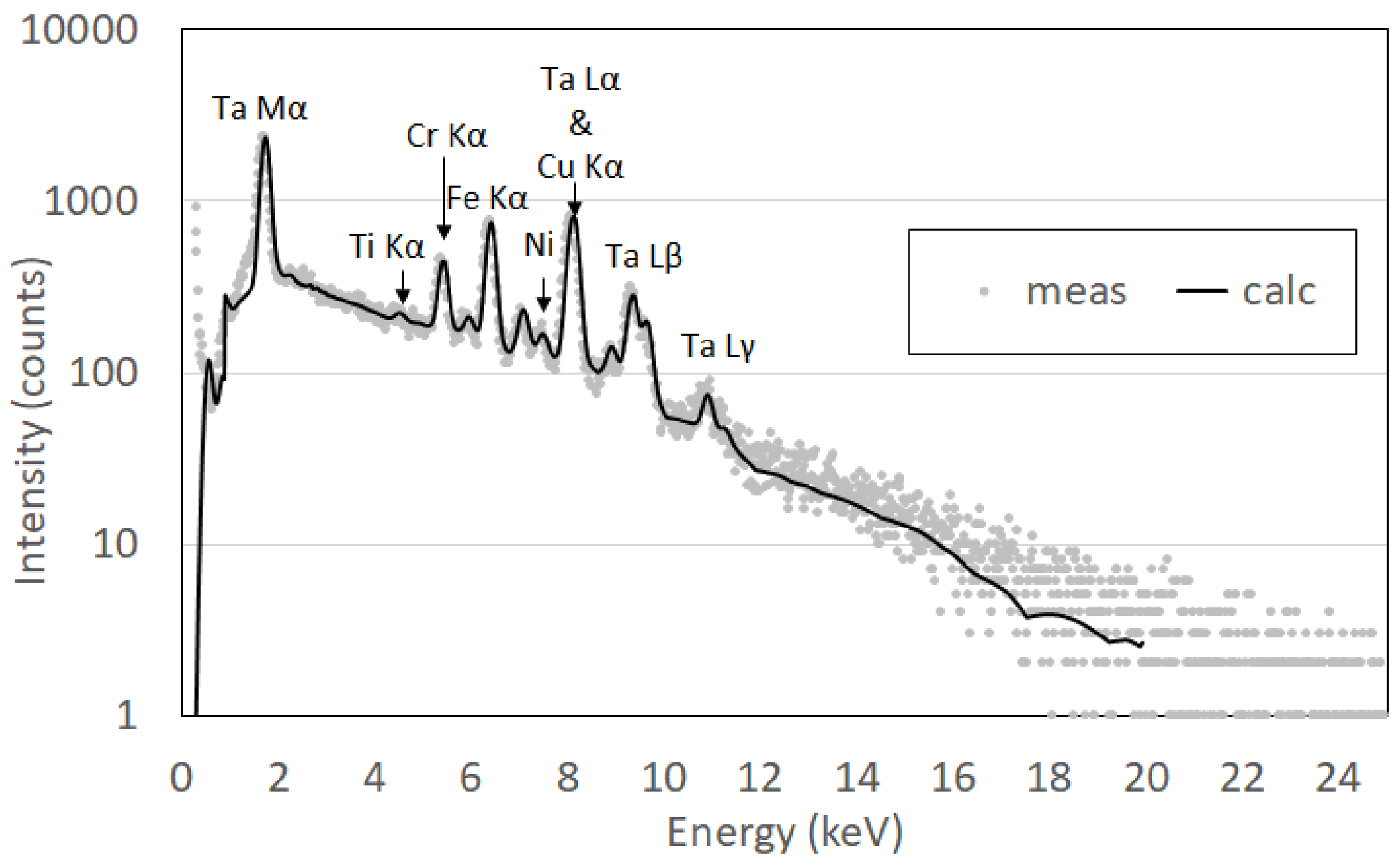

Figure 2: Primary X-ray emission profile fitted using PIQUANT - software used by PIXL. Crystal X-ray lines (Ta K X-rays) and casing lines (Cu, Fe, Cr, Ti) are identified.

Approach:

Observing primary emission (Fig. 2) - cycling ΔT **cold** (25 C) ↔ **hot** (45 / 50 / 55 / 60 C)

1. Vary - pressure 6 / 16 / 26 mTorr in air
2. Vary - crystal separation distances (d) 5.0 / 7.5 / 10.4 mm
3. Build software to automate thermal cycling – LabVIEW GUI (Fig. 3)

FY'18 & '19 Results:

Temp. set-point limit:	50 ° C	→ optimal flux - *40 or 60 C less effective*	Fig. 4
Pressure:	16 mTorr	→ optimal stability & flux	Table 1 and Fig. 5
	26 mTorr	→ optimal E_{max}	Table 1 and Fig. 5
Separation:	5.0 mm	→ optimal flux & E_{max}	Table 1 and Fig. 6
	10.4 mm	→ optimal stability	Table 1 and Fig. 6

Flux emitted ~parallel to crystal face ~1/100th MER APXS

User-defined parameters:
- Output file path
- Number of temperature cycles
- Temperature set-points

Temperature and Integrated Intensity variability with time

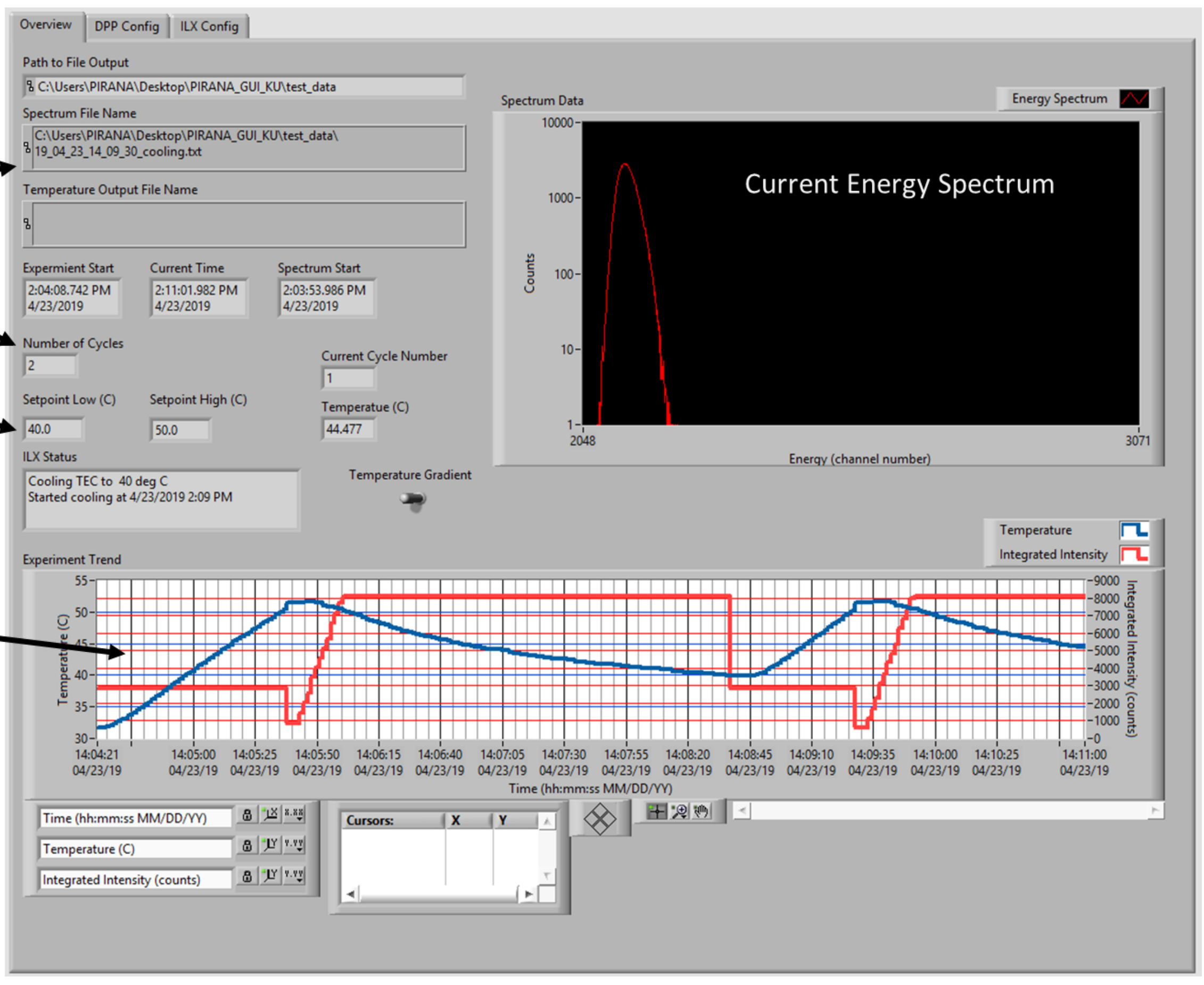

Path to File Output: C:\Users\PIRANA\Desktop\PIRANA_GUI_KU\test_data

Spectrum File Name: C:\Users\PIRANA\Desktop\PIRANA_GUI_KU\test_data\19_04_23_14_09_30_cooling.txt

Temperature Output File Name:

Experiment Start: 2:04:08.742 PM 4/23/2019

Current Time: 2:11:01.982 PM 4/23/2019

Spectrum Start: 2:03:53.986 PM 4/23/2019

Number of Cycles: 2

Current Cycle Number: 1

Setpoint Low (C): 40.0

Setpoint High (C): 50.0

Temperatue (C): 44.477

ILX Status: Cooling TEC to 40 deg C
Started cooling at 4/23/2019 2:09 PM

Figure 3: LabVIEW GUI controls: spectra acquisition, temperature control and monitoring and, operational parameters.

Figure 4: Data from temperature cycling at upper limit set points: 45, 50, 55 & 60 C (4a) showing cumulative flux across 8 cycles (4b) and individual cycle flux counts (4c).

Table 1: Pressure and crystal separation and Pressure variation test results showing mean and spread in data.

	Variable	Mean μ	Std. Dev. σ	Variation σ/μ (%)	Fixed Variables
Separation distance (d) [mm]	10.4	12656	776	6	1 μA, 16 mTorr
	7.5	20839	2051	10	
	5.0	**38331**	**10195**	**27**	
Pressure [mTorr]	26	6022	3508	58	1 μA, d = 10.4 mm
	16	**12656**	**776**	**6**	
	6.1	1841	429	23	

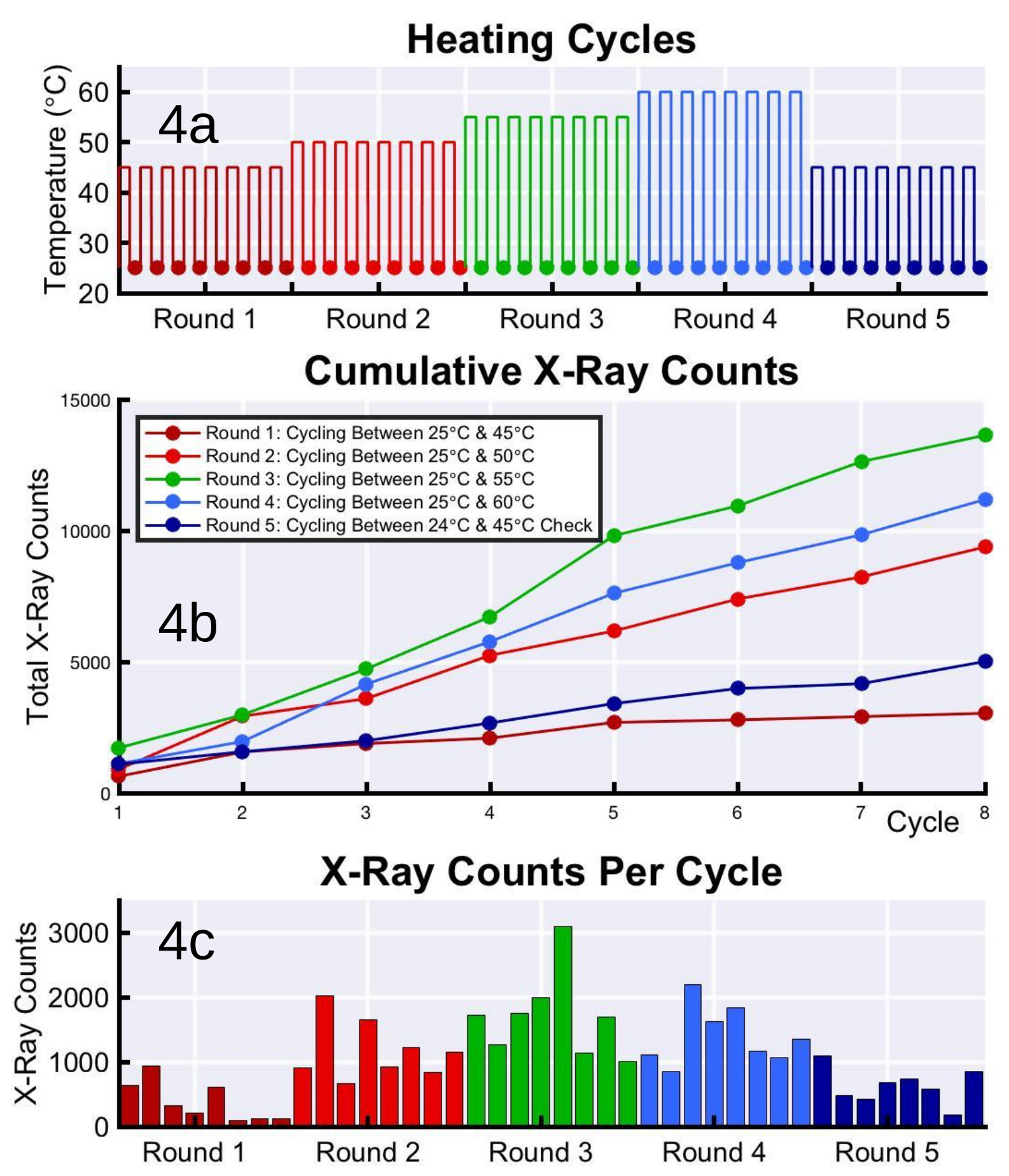

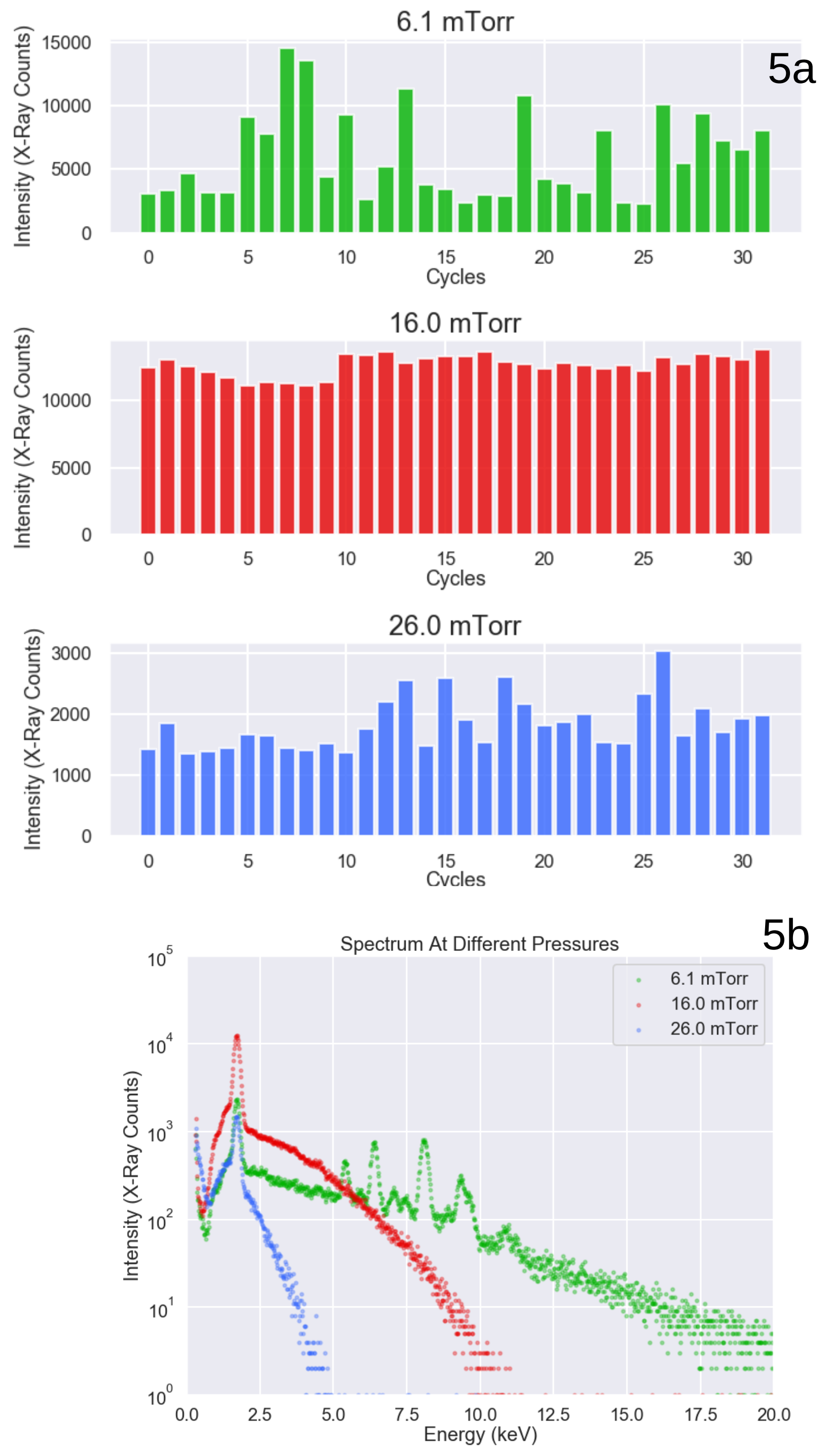

Figure 5: 6, 16 and 26 mTorr air pressure comparison on flux (3a) and maximum energy (keV) (3b).

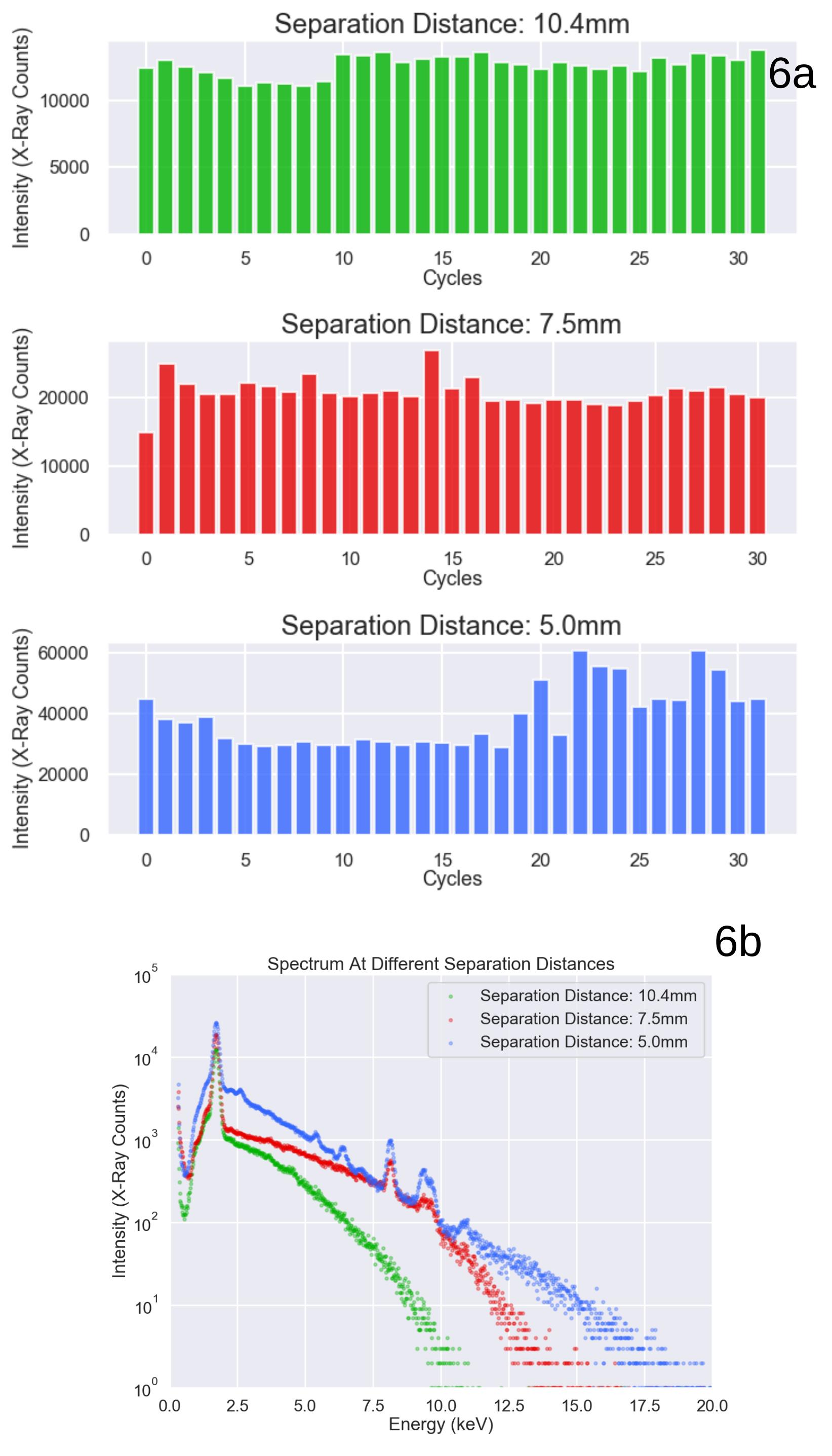

Figure 6: 5, 7.5 and 10.4 mm crystal separation comparison on flux (4a) and maximum energy (keV) (4b).

Conclusions:

Prototype PIRANA results warrant continued development as a reliable X-ray source for future missions. Testing of several variables has illuminated conditions for balancing stability with enhanced flux and maximized energy. Design changes will be considered for further optimization.

Benefits to NASA and JPL:

Development of PIRANA may introduce a new generation X-ray instrument for use onboard exploratory spacecraft. Its **simple design** and **low voltage**, potential **low power** requirements make it advantageous for operation in certain environments (ie. Mars). Any mission, simple to complex, via lander or rover, could utilize this as a source if objectives are realized.

Acknowledgments:

We extend our appreciation to Dr. David Flannery (formerly of JPL) for initiating this task and to summer intern Hannah Munguia-Flores for her assistance on this project.

PI: Dr. Christopher Heirwegh, 1-626-807-5420, Christopher.m.heirwegh@jpl.nasa.gov

1. Lang, S. B., Pyroelectricity: From ancient curiosity to modern imaging tool. Physics Today 58 (2005) 31 – 36.
2. Brownridge, J. D. and Raboy, S., Investigations of pyroelectric generation of x rays. Journal of Applied Physics 86 (1999) 640 – 647.
3. Geuther, J. A. and Danon, Y., High-energy x-ray production with pyroelectric crystals. Journal of Applied Physics 97 (2005) 104916.
4. Kawai, J. et al., X-ray fluorescence analysis with a pyroelectric x-ray generator. X-ray Spectrometry 34 (2005) 521 – 524.
5. https://www.amptek.com/products/x-ray-sources/cool-x-pyroelectric-x-ray-generator
6. Kim, K.J. et al., An Active X-Ray Spectrometer for the SELENE-2 Rover. Trans. JSASS Aerospace Tech. Japan 12 (2014) 35-42.

National Aeronautics and Space Administration

Jet Propulsion Laboratory
California Institute of Technology
Pasadena, California

www.nasa.gov

Poster No. RPC-194